



Modeling cancer immunotherapy: Assessing the effects of lymphocytes on cancer cell growth and motility



R.A. Ramos^a, Jair Zapata^a, C.A. Condat^{b,*}, Thomas S. Deisboeck^c

^a Department of Physics, University of Puerto Rico, Mayagüez, PR 00681, USA

^b IFEG- CONICET and FaMAF, Universidad Nacional de Córdoba, (5000) Córdoba, Argentina

^c Complex Biosystems Modeling Laboratory, Harvard-MIT (HST) Athinoula A. Martinos Center for Biomedical Imaging, Massachusetts General Hospital, Charlestown, MA 02129, USA

ARTICLE INFO

Article history:

Received 5 April 2012

Received in revised form 19 December 2012

Available online 4 February 2013

Keywords:

Tumor model

Cancer growth

Immunotherapy

Lymphocytes

Cell blockade

ABSTRACT

A mesoscopic model is used to describe the effects of lymphocyte activity on a growing tumor. The model yields novel insights into the tumor-immune system interaction. In particular, we found that the presence of a putative chemotactic messenger that helps guide the lymphocytes towards the tumor is not critical to elicit the anti-tumor effects of the immune system, while lymphocytes that block tumor cell migration contribute to limit cancer expansion and thus have a more significant therapeutic impact.

© 2013 Elsevier B.V. All rights reserved.

1. Introduction

An enormous effort has been made in the field of cancer therapies, but the results are still not satisfactory; in particular, although immunotherapy holds promise and has shown a few striking successes [1,2], there remain many aspects of the interaction between the immune system and a tumor that are not well understood. Modeling of the immunogenic response to a tumor has helped us to understand these processes better, but it has been usually limited to zero-dimensional models, where the total distribution of the various populations, but not their anatomical distribution has been considered [3–11]. Since a tumor is a complex, self-organizing system whose evolution is mediated by such physical phenomena as migration, growth, and morphological instability [12,13], a physicist's approach can help us to understand the spatial features of cancer growth and the modifications brought about by therapy. The mathematical toolkit of the physicist, which includes nonlinear differential equation systems and spatially extended numerical simulations, is useful for a precise formulation of the relevant processes. This is the approach taken in this work.

The traditional way of modeling cancer with the direct use of differential equations is summarized, for example, in the book of Adam and Bellomo [12]; for a modern use of these methods in therapy, see Ref. [14]. In the last decade, several mesoscopic models have provided new insights into the dynamics of cancer growth [15–18]. More recently, cancer modelers have started to apply these methods to study the interaction between the tumor and the immune system [19–21].

The immune response to cancer is summarized, for instance, in the book by Wodarz and Komarova [22]. Multiple therapeutic approaches have been used, with uneven results, to prime the immune system against a tumor [23–25]. Here we will consider only adaptive cellular immune responses. In brief, tumor cells are thought to be immunogenic, i.e. they display on their surfaces cancer-specific proteins (the antigen), which can elicit an immune reaction. That is, specific cytotoxic

* Corresponding author. Tel.: +54 351 4334051; fax: +54 351 4334054.

E-mail address: condat@famaf.unc.edu.ar (C.A. Condat).

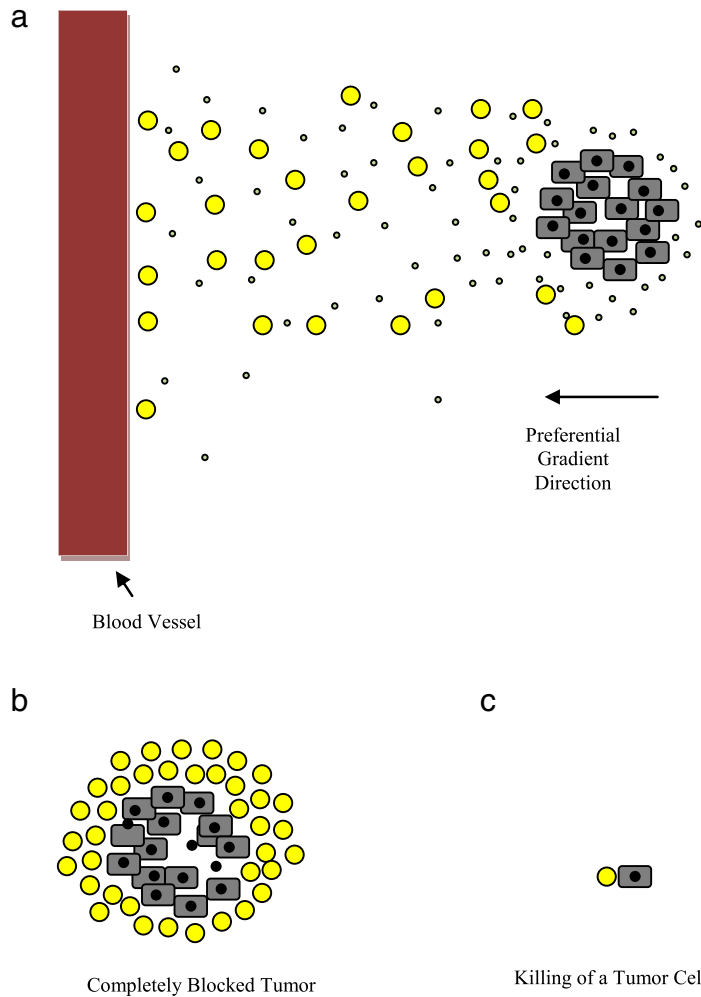


Fig. 1. (a) Lymphocytes (disks) emerging from the circulatory system detect a “messenger” (black dots) gradient that triggers lymphocyte chemotaxis towards the tumor. This may lead to the formation of a lymphocyte barrier (b) that contains tumor progression (b). Tumor cell killing proceeds simultaneously (c).

T-lymphocytes (CTLs) are able to recognize these cancer proteins displayed in conjunction with major histocompatibility complex (MHC) molecules on a tumor cell surface. Recognition of the protein–MHC complex by the CTL triggers the release of apoptosis-inducing molecules.

In this paper we focus on two phenomena that can only be studied with a spatio-temporal model: the effectiveness of lymphocyte-guiding messenger molecules and the efficacy of a physical, invasion-inhibiting, blockade of the advancing cancer front by the lymphocytes. Lymphocytes can be oriented towards the tumor by chemotaxis or haptotaxis. We will consider the first phenomenon, imagining that lymphocytes can follow the chemotactic trail left by messenger molecules emitted by cancer cells. The existence of these messenger molecules has been recognized for a long time [26,27]. We would like to test if, by improving CTL tumor-homing capacity, these molecules can contribute to substantially enhance the efficacy of antitumoral immune activity. On the other hand, the observation of leukocytes rosettes surrounding the tumoral cells [28] and the observation that neutrophils position themselves to hamper cancer cell migration [29] suggest that one important effect of immune cells in cancer may be to surround the cancer cells to restrict the tumor expansion. We will therefore assume that surrounding lymphocytes act on tumor cells in two different but complementary ways: by lysing or killing them and by blocking their invasion of surrounding tissue. The main processes are schematically depicted in Fig. 1.

The mesoscopic model to be used in our analysis is an extension of that of Scalerandi and co-workers [15,30,31]. In this model, some rules formulated at the cell level are implemented as difference equations on a lattice. The equations are then solved using numerical simulations. Among other results, this procedure led to the reproduction of MRI data from real tumors [32] and to the description of cell shedding by multicellular tumor spheroids (MTS) [33]. In the case of the MTS, the mesoscopic model has also been related to its macroscopic counterpart through an intermediate model [34]. In the present work, lymphocytes will be assumed to enter the region containing the affected tissue through the circulatory system, and

be chemotactically guided towards the tumor. The guidance is provided by a messenger molecule that is generated by the cancer cells; such a chemotactic factor could be a peptide [35] or a protein [36]. To apply the procedure of Ref. [15] to model the tumor–immune system interaction, we need to establish new rules for the additional populations, i.e., the lymphocytes and the messengers.

There are therefore two hypotheses that we will test with our model. The first is that the guidance of lymphocytes towards the tumor renders the immune response significantly more effective. The second is that the physical blockade of the tumor cells by lymphocytes proposed by Brú and coworkers as an important effector of immune system action [29] is actually an efficient mechanism to limit tumor propagation. As we shall see, while the messenger effect is relatively weak (except, perhaps at the earliest tumor stages), the formation of a physical barrier can crucially modify the dynamics of tumor growth.

2. Methods

2.1. Tumor rules

Let us begin by reviewing the basic growth model (no immune system involved) as described in Ref. [15]. The piece of originally healthy tissue under consideration is discretized and the nutrient distribution is left to evolve until it reaches its steady state. Free nutrient diffuses from one or more blood vessels with a diffusion coefficient α . Healthy cells absorb free nutrient at node \vec{i} at a rate $\gamma_N h(\vec{i})$, where $h(\vec{i})$ is the local cell concentration. A cancer seed c_0 is then introduced and made to evolve under the following rules:

(T1) *Feeding*. Cancer cells absorb free nutrients at node \vec{i} at the rate

$$\gamma(\vec{i}) = \gamma_\infty \left[1 - e^{-\Gamma p(\vec{i})} \right], \tag{1}$$

where Γ is an affinity parameter, which we will take equal to unity. The absorption rate is proportional to the local free nutrient concentration $p(\vec{i})$ at low concentrations but it saturates at high concentrations. Absorbed nutrients will be called bound nutrients.

(T2) *Consumption*. The bound nutrient, whose concentration is $q(\vec{i})$, is consumed by cancer cells at the rate

$$\beta(\vec{i}) = \beta_\infty \left[1 - e^{-q(\vec{i})/c(\vec{i})} \right], \tag{2}$$

where the denominator $c(\vec{i})$ has been included in the exponent because each cell can consume only its own bound nutrient.

(T3) *Death*. When the average amount of bound nutrient per cell, $q(\vec{i})/c(\vec{i})$, falls below a given threshold Q_D , a fraction $r_D c(\vec{i})$ of cancer cells dies.

(T4) *Mitosis*. A high concentration of bound nutrient may trigger cell replication. This is supposed to occur if $q(\vec{i})/c(\vec{i})$ exceeds a mitosis threshold Q_M ($Q_M > Q_D$); then, a fraction $f_{i,j}$ of healthy cells are effectively replaced by new cancer cells. This fraction is given by,

$$f_{i,j} = h(\vec{i}) + \left[r_M c(\vec{i}) - h(\vec{i}) \right] \Theta \left[r_M c(\vec{i}) - h(\vec{i}) \right]. \tag{3}$$

Where $\Theta(x)$ is Heaviside's step function and r_M is a constant.

(T5) *Migration*. A cell that senses a low nutrient level in its neighborhood tends to migrate. If P_D is a free nutrient migration threshold, we assume that the cell moves, with a migration rate $\tilde{\alpha}$ if $p(\vec{i})/c(\vec{i}) < P_D$. We assume that healthy tissue cells are eliminated i.e. replaced by the invading cancer cells.

2.2. Lymphocyte rules

(L1) *Messenger generation*. Cancer cells generate a molecular messenger, representing a protein, that diffuses, with a diffusion coefficient α_m , through the tissue. These molecules are assumed to leave the tissue when they reach its edges, and have a mean lifetime τ_m , after which they degrade. Their presence defines a field that orients the lymphocytes towards the messenger sources, i.e., the regions with high cancer cell densities. The messenger concentration $m(\vec{r}, t)$ satisfies the equation,

$$\frac{\partial m(\vec{r}, t)}{\partial t} = -\frac{m(\vec{r}, t)}{\tau_m} + \alpha_m \nabla^2 m(\vec{r}, t) - Gm(\vec{r}, t) l(\vec{r}, t) + Kc(\vec{r}, t), \tag{4}$$

where G and K are, respectively, the messenger–lymphocyte binding coefficient and the messenger generation rate, and $l(\vec{r}, t)$ is the lymphocyte concentration. (For brevity, in this section we give the continuum versions of the equations.)

(L2) *Lymphocyte migration.* Since the immune reaction is not immediate, a delay t_1 must be implemented between the introduction of the cancer seed and the onset of the response. Once a lymphocyte has penetrated the affected area, it migrates under the influence of the messenger concentration gradient, with a chemotactic coefficient χ . If τ_l and α_l are, respectively, the mean lifetime and migration coefficient of the lymphocytes, their concentration satisfies the equation,

$$\frac{\partial l(\vec{r}, t)}{\partial t} = -\frac{l(\vec{r}, t)}{\tau_l} + \alpha_l \nabla^2 l(\vec{r}, t) - \nabla \cdot [l(\vec{r}, t) \nabla m(\vec{r}, t)]. \quad (5)$$

If $\chi = 0$, lymphocyte diffusion is isotropic, but a nonzero χ favors lymphocyte motion towards the messenger source, i.e., the live tumor cells.

(L3) *Lymphocyte attack.* We describe the action of the lymphocytes on the cancer cells through the equation

$$\frac{\partial c(\vec{r}, t)}{\partial t} = -bl(\vec{r}, t)c(\vec{r}, t) \quad (6)$$

where b , the *killing efficacy*, is a parameter that characterizes the lymphocyte efficiency to destroy cancer cells. Lymphocytes are assumed to kill multiple targets [37]. If they were to be inactivated by their interaction with the cancer cells, a suitable negative term should be added to Eq. (5).

(L4) *Blockade.* High lymphocyte concentrations are assumed to obstruct the passage of cancer cells. If $\left(\vec{i}\right) > \Theta_B$, where Θ_B is a blocking threshold, cancer cells cannot migrate to node \vec{i} . Of course, a cell taking part in the blockade can also kill a neighboring cancer cell: both effects occur simultaneously once this rule is implemented.

We remark that, although in the simulations presented in this paper all lymphocytes enter the system through the blood vessel, the model can be easily modified to account for on-site proliferation.

2.3. Initial and boundary conditions

We represent the tissue of interest by a two-dimensional square grid, with lattice constant Δ . Although the use of discretized equations permits a great generality in the choice of the tissue properties, for simplicity we choose a square tissue area, with the nutrients being supplied by a single capillary located at the lower edge of the lattice. The nutrient concentration in the blood vessel is constant, $\left[\vec{i} = (i, 0), t\right] = P_0$. Periodic boundary conditions are used for the right and left boundaries and absorbing conditions for the upper edge. If we use a grid with 100×100 node points on a $1 \text{ cm} \times 1 \text{ cm}$ tissue area, the discretization interval is $\Delta = 100 \mu\text{m}$ and each node contains about 100 cells. Following the local interaction simulation approach of Scalerandi et al. [15], the molecular and cellular concentrations are modified by the local conditions at each step.

To ensure stability, the time discretization step τ must satisfy $\tau \leq \Delta^2/2$. On the basis of many simulations we have chosen $\tau = 0.05$.

2.4. Therapy

Adaptive immunotherapy increases the number of stimulated lymphocytes available to attack the cancer cells. In current vaccination studies, these autologous lymphocytes may be either activated *in vivo* or activated *in vitro* with tumor-associated antigen and then transferred to the patient (for a recent review, see e.g. Ref. [38]); for the purpose of this study here we will assume that in all cases they arrive at the region containing the tumor via the circulatory system. To model immunotherapeutic action, we thus increase the lymphocyte concentration in the tumor-feeding vessel. This is done through a modification in the boundary condition. If l_0 is the baseline lymphocyte concentration and $f(t)$ is a function that represents the therapy protocol, we write,

$$l(\vec{i} = (i, 0), t) = l_0 + f(t). \quad (7)$$

3. Results

In the absence of an immune system, the growth is nutrient-controlled and has the features known from previous work: an inner necrotic core rapidly develops; it is surrounded by a layer of quiescent cancer cells and a rim of proliferating cells. It was shown in Ref. [15] that various growth modes could be adequately described by the basic model in the absence of an immune reaction. Here we have chosen a set of parameters that ensures a relatively fast, symmetric growth of the “bare” tumor, i.e., the one without an immune system, so that a complicate geometry does not obscure the interpretation of the immune system action. It is possible, of course, to study the evolution of other tumor types; for instance, a sharp reduction of

Table 1

Tumor growth parameters. Here c_0 is the cancer cell concentration at the seed node and q_0 the initial concentration of bound nutrient there.

P_0	c_0	q_0	α	γ_N	γ_{as}	β	$\tilde{\alpha}$	Q_D	Q_M	P_D	r_D	r_M
0.7	0.2	0.01	0.25	0.0002	0.52	0.08	0.1	0.057	0.3	0.4	0.2	0.25

Table 2

Messenger and lymphocyte parameters.

α_m	τ_m	K	G	α_l	τ_l	b	χ	F	A	a	T
2.0	1000	0.01	0.01	2.0	1000	0.1	10.0	100	100	10	575

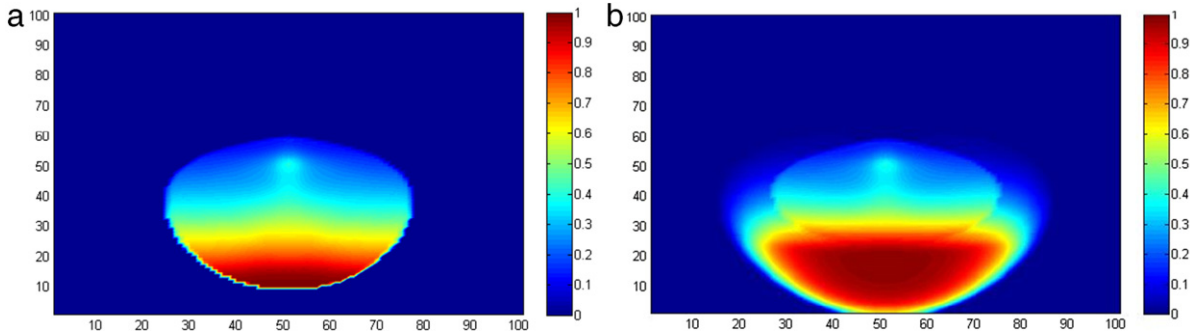


Fig. 2. Simultaneous snapshots of the apoptotic cancer cell distribution (a) in the absence and (b) in the presence of immune reaction. In these simulations lymphocytes are assumed to kill cancer cells, but they do not restrict (block) their motion. Parameters are as in Tables 1 and 2. Although the original mass of dead tissue has been reduced in volume by lymphocyte activity, a large area of tissue destruction emerges in the direction of the blood vessel, consistent with reports in the literature about the appearance or exacerbation of peritumoral edema in some patients with high grade glioma following treatment with interleukin and interferon [40]. Live cancer cells (not shown) are mostly concentrated at the perimeter of the dead cell region and are especially active in the region close to the nutrient source. The initial immune reaction thus favors tumor expansion and re-growth and, as a consequence, normal tissue destruction.

the migration rate $\tilde{\alpha}$ would lead to a very asymmetric, slow-growing bare tumor, but the ensuing qualitative changes should not be dramatic. We have studied the effects of (a) having an active immune system represented by CTLs, (b) implementing the immunotherapy, and (c) implementing the blockade rule, L4. To do this, we have used the parameter values in Table 1.

3.1. Immune response

We start by considering the immune reaction in the absence of therapy. After the response delay t_1 , the lymphocytes enter the tissue through the vessel, and follow the messenger gradient towards the cancer cells, which they attack. As a consequence, the number of live cancer cells decreases markedly and growth in the directions parallel and opposite to the blood vessel slows; the tumor, however, continues to grow towards the nutrient source [see #5 in Conclusions]. The number of dead cancer cells increases and its distribution gets more lopsided towards the blood vessel (compare panels (a) and (b) in Fig. 2). The number of healthy cells is also reduced. The reason for this somewhat surprising behavior is the increase in the nutrient quantity available to the smaller number of surviving cancer cells. These multiply more rapidly because of the absence of competition, an effect first noticed in Ref. [21], displacing normal tissue cells (this process is a direct consequence of rules T4 and T5). *In situ* lymphocyte proliferation (not considered here), if it occurs, could have a beneficial effect, as it might constrain cancer re-growth.

An important objective is to determine the relevance of the messenger for the immune reaction. This is studied by making extensive sweeps of the messenger parameters: α_m , τ_m , G , K , and χ . Fig. 3(a) and (b) show the effects of modifying α_m and τ_m , respectively. Both an increase in the messenger diffusion coefficient and a lengthening in its lifetime decrease the number of live cancer cells, but the result is not very sensitive to variations in these parameters. The dependence on G and K is also weak. What makes the difference is the number and activity of the lymphocytes; they eventually find and destroy cancer cells. The messenger seems to play only a secondary role. This is confirmed by Fig. 3(c), which shows the time dependence of cancer cell number for various values of the chemotactic strength χ , including $\chi = 0$ (no messenger effect).

The dependence of the efficiency of immune action on the lymphocyte parameters is much stronger. An increase in the lymphocyte migration coefficient α_l decreases the number of cancer cells (see Fig. 4(a)). Snapshots (not shown) indicate that the distributions of cancer and dead cells are also modified, the cancer cells forming a thicker, lower-concentration shell for high values of α_l . Increasing the killing efficacy b of the lymphocytes strongly reduces the number of cancer cells (Fig. 4(b)); unfortunately no concomitant reduction of the damage to the normal tissue is observed, as shown but the total dead cell

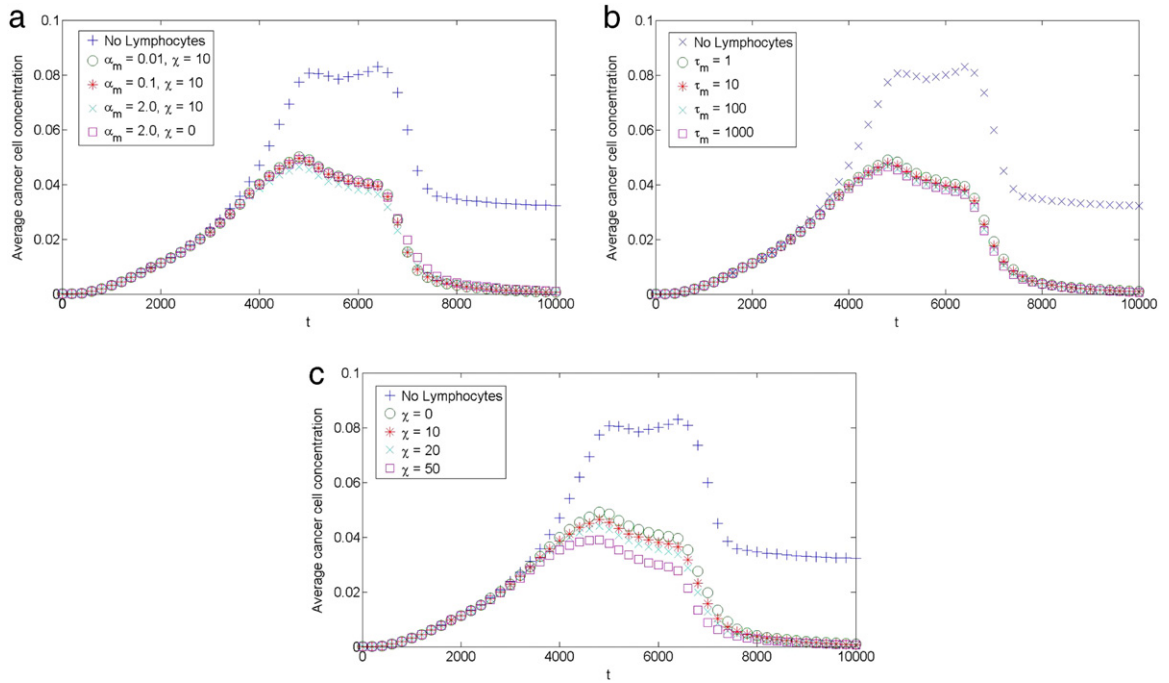


Fig. 3. Time evolution of the average cancer cell concentration for various values of (a) the messenger diffusion coefficient α_m , (b) the messenger lifetime τ_m , and (c) the chemotactic coefficient χ . Other parameters are as in the Tables. The first peak in the figures corresponds to the arrival of the first cancer cells at the blood vessel. In all cases, the anti-cancer efficacy is enhanced at long times. Lymphocyte efficacy is only weakly dependent on the chemical cue parameters.

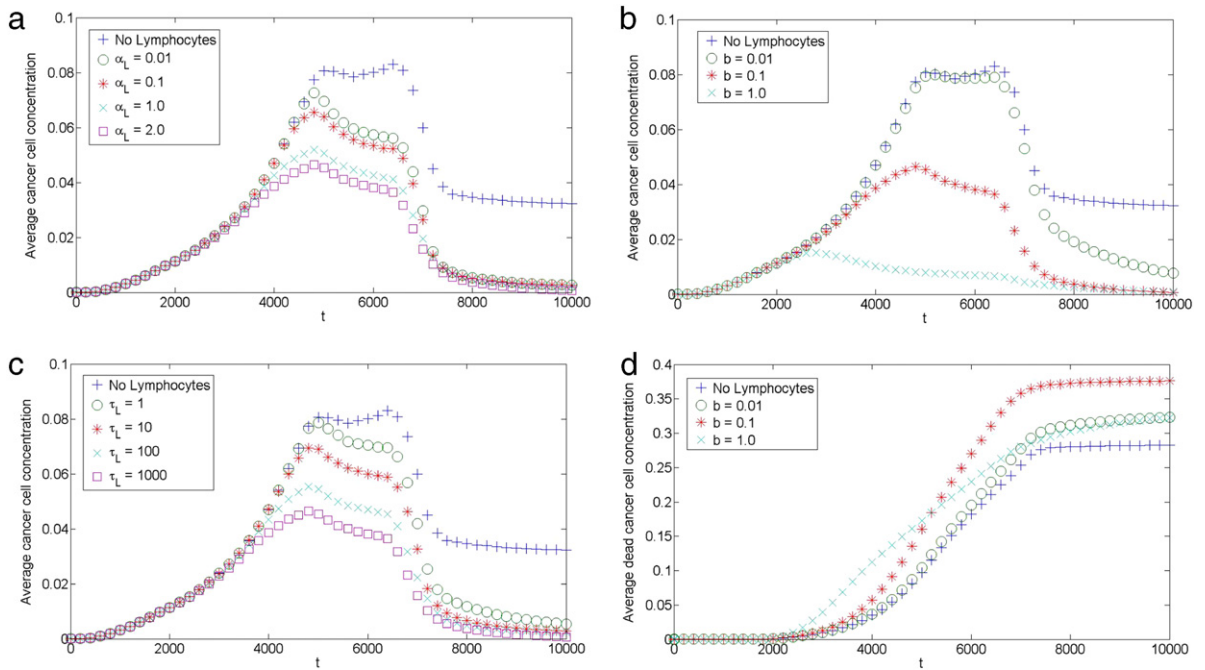


Fig. 4. Time evolution of the average cancer cell concentration for various values of (a) the lymphocyte migration coefficient α_L , (b) the lymphocyte killing efficacy b , and (c) the lymphocyte lifetime τ_L . (d) Time evolution of the average dead cancer cell concentration for various values of b .

count (Fig. 4(d)). Indeed, for an intermediate value (1) of the parameter b , tumor-induced tissue destruction is considerably increased. The viable cancer cells form a very thin layer that extends in the direction parallel to the feeding vessel. Increasing

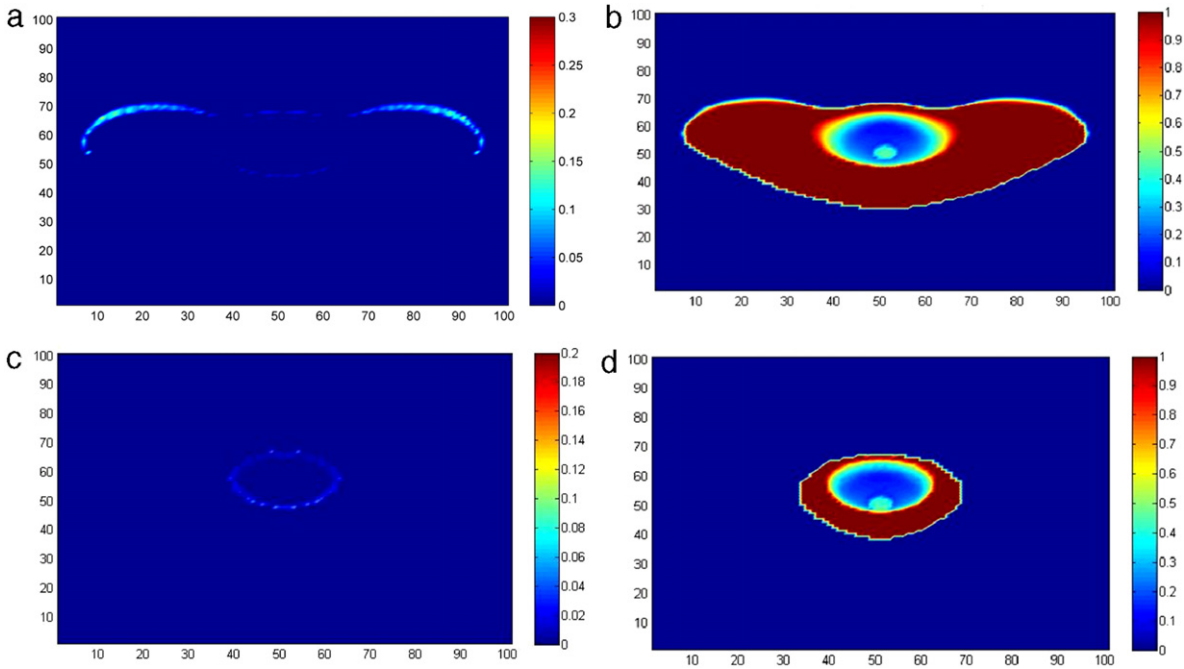


Fig. 5. Effects of strong therapeutic action and blockade. Snapshots of (a) live cell and (b) dead cell distributions, with no blockade implemented. Panels (c) and (d): same as (a) and (b), respectively, but including blockade with $\varrho_B = 0.5$. From (c) and (d) we see that the tumor has been reduced to a small necrotic remnant by the combined action of blocking and killing. Tumor parameters are as in Tables 1 and 2.

the lymphocyte mean lifetime τ_l decreases the number of live cancer cells, but this effect is weaker than changing either α_l or b (Fig. 4(c)). The value of τ_l is, on the other hand, important to determine the time between therapy applications.

3.2. Immunotherapy

To investigate the influence of immunotherapy on cancer growth, we implement Eq. (7) at times $t > t_2$, where t_2 is the time when the immune treatment was started. If the therapy is administered following a periodic protocol, the important parameters are the integrated increase F in the lymphocyte concentration in the blood vessel (this is the time integral of $f(t)$ over a single period) and the period T . We have tried various forms for the periodic function $f(t)$ (cosine, square pulse, sawtooth, etc.), but no substantial improvement is achieved by modifying the function shape. On the contrary, the influence of the “dose” F is strong: a high value of F leads to a steep decrease in the number of cancer cells; although the overall tumor volume is not substantially decreased, the tumor becomes more compressed along the horizontal axis. We note that testing these influences has biological relevance as it has been shown that e.g. the length of *in vitro* anti-CD3 stimulation, and the dose and timing of IL-2 administration *in vivo* results in different circulating leukocyte populations after adaptive T-AK infusion [39]. In the following, we use an exponential therapy protocol:

$$f(t) = A \left[1 - \exp\left(-\frac{a}{T}t'\right) \right] \quad \text{if } F \sin \omega T > 0 \tag{8a}$$

and

$$f(t) = A \exp\left(-\frac{a}{T}t'\right) \quad \text{if } F \sin \omega T < 0. \tag{8b}$$

Here a is a real number, A is the maximal lymphocyte concentration increase at the blood vessel, and $t' = \text{module}(t, T/2)$.

Panels (a) and (b) in Fig. 5 exhibit the surviving rim of cancer cells and the very deformed necrotic core, after a very long time. Fig. 6(a) and (b) show, respectively, the effect of therapy on the total concentration of cancer and dead cells. Although the number of cancer cells is much reduced, they are not completely eliminated. Initially, the therapy increases the damage caused by the tumor to the tissue through the already described process of partially destroying cancer cells while allowing the survivors to reproduce rapidly at the expense of the normal tissue; however, at longer times it should have a beneficial value (if the affected organ survives) because the number of remaining healthy cells is much larger. The reason is that surrounding lymphocytes delay and constrain cancer cell invasion of the surrounding tissues.

The influence of modifying T is strong only if $T > \tau_l$. If we select $T \gg \tau_l$, the therapy fails because the tumor restarts a rapid growth (very few reproductive cells compete for a lot of nutrients, which ensures rapid mitosis).

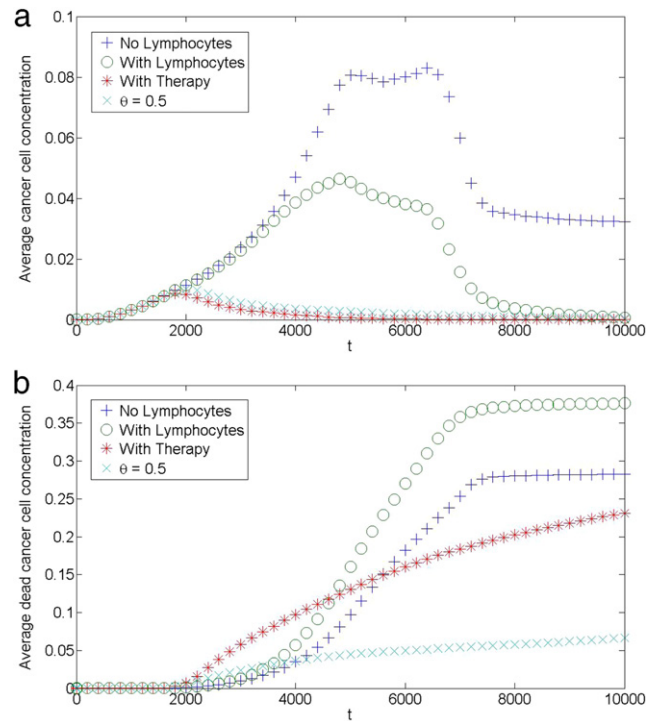


Fig. 6. Time evolution of (a) the average live cancer cell concentration and (b) the average dead cancer cell concentration in the absence of an immune system (+), with spontaneous (i.e., no therapy) immune action starting at $t_1 = 500$ (o), with immune therapy starting at $t_2 = 500$ (*), and including rule L4—lymphocytes block cancer cell migration (\times). A therapy with killing lymphocytes that do not obstruct cancer cell migration decreases the instantaneous number of cancer cells, but does not eliminate them completely. The blocking property of lymphocytes, embodied in rule L4, is crucial for therapeutic success.

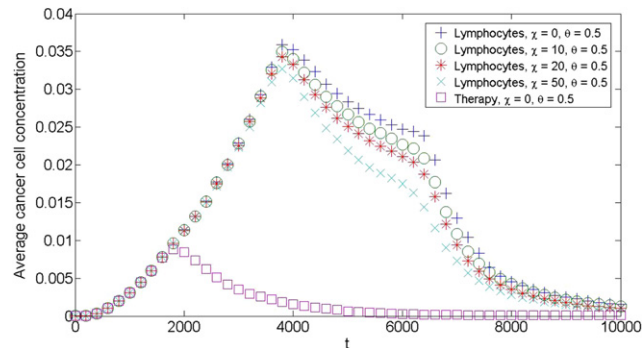


Fig. 7. Spontaneous immune response is ineffective, even if the blocking rule is implemented. The upper curves were obtained by varying the chemotactic coefficient and implementing rule L4, in the absence of therapy. The lowest curve was obtained by applying therapy and the blocking rule, but with no chemotaxis.

3.3. Blockade

The effect of the blockade can be seen in panels (c) and (d) in Fig. 5, and in Fig. 6, where rule L4 (lymphocyte obstruction of cancer cell motility) was implemented. Cancer cells become surrounded by lymphocytes and tumor expansion stops. At the time of observation very few cancer cells survive, and the damage to the tissue is effectively reduced, as compared with panel *b* (no blockade). A thick, confined necrotic shell surrounds a region containing mostly normal cells. This is the result of fast initial tumor expansion (mediated by the initial lymphocyte action) (see Fig. 6(b)) followed by the formation of an efficient barrier of killing/blocking lymphocytes.

It is interesting to note that the lymphocyte blockade becomes truly efficient only when it is combined with therapeutic action. This is shown in Fig. 7, where we see that implementation of the blocking rule in the absence of therapy does not significantly reduce the number of live cancer cells. Such a reduction is obtained when we combine therapy and the blocking rule, even if we ignore chemotaxis (lowest curve in Fig. 7).

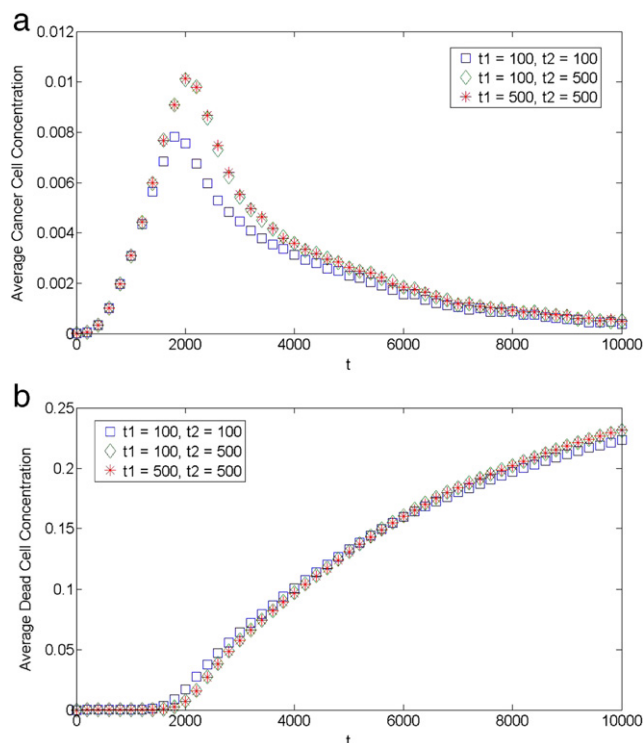


Fig. 8. Response to time delays. (a) Cancer cell concentration and (b) dead cell concentration as functions of the time, for the values of the delays in the onset of the immune response (t_1) and in the application of therapy (t_2) indicated in the figure.

Two time lags have been incorporated into this model. There is a delay t_1 between the apparition of the cancer seed and the onset of the immune response and there is a time t_2 elapsed before the start of the therapy. The effects of time delays on zero-dimensional systems are well known and are discussed in mathematical biology textbooks [41] and in the more specialized literature [42]. In the case of the interaction between a tumor and the immune system, these effects have been recently discussed in detail by D'Onofrio and coworkers, who show, for instance, that a Hopf bifurcation with the consequent loss of stability may emerge in the case of large delays in the proliferation rate [43]. These authors also considered distributed delays, which may yield resonance peaks. Much less is known about the effect of delays on the evolution of extended systems, such as the one considered here, where many different small time lags are implicit in the cell displacements. This distribution of time lags is likely to obscure any sharp effects that may be caused by fixed delays in the onsets of various processes. In Fig. 8 we present results obtained by changing the values of t_1 and t_2 . It is clear that a modest change in t_1 does not generate any significant consequences. The delay in the time of therapy application, t_2 , has a somewhat stronger but not unexpected effect: there is an enhancement of the early growth in the number of cancer cells and there is a long-time increment in the number of dead cells, because of the increased pool of available cancer cells.

4. Conclusions

Many features of the interaction between cancer and immune system have not yet been completely elucidated. A mesoscopic model that includes space dependence has proved to be useful to quantitatively investigate some aspects of this interaction. In particular, we can conclude that:

1. Immune system activity per se decreases tumor size, but does not delay the remaining tumor cells' spatial advance towards the nutrient source, i.e. the immune reaction to the primary tumor does not slow the onset of the invasive and metastatic processes. The number of surviving healthy tissue cells is effectively decreased by the immune action, since lymphocyte attack reduces the number of intraspecies competitors for surviving cancer cells—new cancer cells appear at the expense of preexisting normal tissue cells (tumor recurrence); however, most of these new cancer cells are, in due course, rapidly destroyed by lymphocytes. We remark that we have included only the damage to the normal tissue due to tumor expansion. Possible direct toxic effects of the immune cells on the normal tissue may be important and will be investigated with a straightforward modification of the current model.

2. The putative chemical messenger or chemotactic cue does not critically enhance the response. It remains to be considered whether haptotactic guidance, which could be modeled as facilitated migration, could be more effective.

3. Tumor growth is very sensitive to lymphocyte parameters. In particular, increasing the killing efficacy strongly reduces the number of cancer cells, but without reducing the tumor volume (thus increasing the central necrosis size). Since, without

the blockade effect, immune system action is not effective against a well-fed, fast growing tumor, we have not included lymphocyte inactivation by the action of cancer cells in our model. Lymphocyte inactivation would essentially imply a weaker immune response. It could be important to ensure the thriving of some slow-growing tumors and it could be easily modeled by the addition of a term proportional to $-l(\vec{r}, t) c(\vec{r}, t)$ to the right-hand side of Eq. (5).

4. As Fig. 6(b) shows, immunotherapy may indirectly increase the damage caused by the (remnant and recurrent) tumor to the normal tissue at short times, but at long times therapeutic efficacy persists and this damage is smaller than in the cases where no therapy has been applied. This relative decrease in normal tissue destruction at long times is much more intense if rule L4 (blocking of cancer cell migration) is implemented. Note that in the case of Fig. 6(b) the total volume of the affected tissue has been reduced to less than one third of what it would have been if rule L4 had not been implemented. By strongly limiting the possibility that mobile cancer cells reach the circulatory or lymphatic systems, the blockade effect could also be efficient to stop or delay the onset of metastasis. This agrees with the observations of Brú and co-workers [29].

5. Cancer growth is driven towards the nutrient source; therefore it would be advisable to include an adjuvant anti-migratory agent in a possible therapeutic program. This agent would potentiate the lymphocyte blocking effect, contributing to stop tumor growth.

6. Moderate delays in the onset of the immune response or in the application of therapy do not lead to dramatic changes in the outcome of the tumor–immune system interaction. However, the general problem of delays in extended systems deserves additional research.

For this study we have chosen a symmetric, fast growing “bare” tumor. It would be possible, of course, to study the evolution of other tumor morphologies; for instance, a sharp reduction of the migration rate $\tilde{\alpha}$ would lead to a very anisotropic, slow-growing bare tumor, the main predicted effect being a strengthening of the lymphocyte blockade.

In summary, our results indicate that killing cancer cells may not by itself be a good therapeutic strategy to prevent recurrence. Rather, highly-efficient killing of cancer cells should be complemented by treatments that either enhance rosette formation around active tumor regions or otherwise inhibit cancer cell migration. Our findings therefore support the use immunotherapy where stimulated CTLs target cancer cells to inhibit motility and promote cell lysis. The possibility that immunotherapeutic action is potentiated by in situ CTL proliferation is currently under study.

Acknowledgments

This work was supported by SECyT-UNC, ANPCyT (PICT 2205/33675), and CONICET (Argentina) through grant PIP 6311/05. CAC thanks the University of Puerto Rico for its hospitality.

References

- [1] H.W. Herr, A. Morales, History of bacillus Calmette-Guerin and bladder cancer: an immunotherapy success story, *J. Urol.* 179 (2008) 53–56.
- [2] F.S. Hodi, et al., Improved survival with Ipilimumab in patients with metastatic melanoma, *N. Engl. J. Med.* 363 (2010) 711–723.
- [3] D. Kirschner, J.C. Panetta, Modeling immunotherapy of the tumor–immune interaction, *J. Math. Biol.* 37 (1998) 235–252.
- [4] F. Nani, H.I. Freedman, A mathematical model of cancer treatment by immunotherapy, *Math. Biosci.* 163 (2000) 159–199.
- [5] O. Sotolongo-Costa, L. Morales Molina, D. Rodríguez Pérez, J.C. Antoranz, M. Chacón Reyes, Behavior of tumors under nonstationary therapy, *Physica D* 178 (2003) 242–253.
- [6] H.P. De Vlarar, J.A. González, Dynamic response of cancer under the influence of immunological activity and therapy, *J. Theoret. Biol.* 227 (2004) 335–348.
- [7] A. D’Onofrio, A general framework for modeling tumor–immune system competition and immunotherapy: Mathematical analysis and biomedical inferences, *Physica D* 208 (2005) 220–235.
- [8] L.G. De Pillis, W. Gu, A.E. Radunskaya, Mixed immunotherapy and chemotherapy of tumors: modeling, applications and biological interpretations, *J. Theoret. Biol.* 238 (2006) 841–862.
- [9] B. Piccoli, F. Castiglione, Optimal vaccine scheduling in cancer immunotherapy, *Physica A* 370 (2006) 672–680.
- [10] C. Cattani, A. Ciancio, Qualitative analysis of second-order models of tumor–immune system competition, *Math. Comp. Modelling* 47 (2008) 1339–1355.
- [11] L.G. De Pillis, et al., Mathematical model creation for cancer chemo-immunotherapy, *Comput. Math. Methods Med.* 10 (2009) 165–184.
- [12] J.A. Adam, N. Bellomo (Eds.), *A Survey of Models for Tumor–Immune System Dynamics*, Birkhäuser, Boston, 1997.
- [13] T.S. Deisboeck, G.S. Stamatakos (Eds.), *Multiscale Cancer Modeling*, Taylor & Francis, Boca Raton, 2011.
- [14] E.S. Norris, J.R. King, H.M. Byrne, Modelling the response of spatially structured tumours to chemotherapy: drug kinetics, *Math. Comp. Modelling* 43 (2006) 820–837.
- [15] M. Scalerandi, A. Romano, G.P. Pescarmona, P.P. Delsanto, C.A. Condat, Nutrient competition as a determinant for cancer growth, *Phys. Rev. E* 59 (1999) 2206–2217.
- [16] A.R. Kansal, S. Torquato, G.R. Harsh IV, E.A. Chiocca, T.S. Deisboeck, Simulated brain tumor growth dynamics using a three dimensional cellular automaton, *J. Theoret. Biol.* 203 (2000) 367–382.
- [17] S.C. Ferreira Jr, M.L. Martins, M.J. Vilela, Reaction–diffusion model for the growth of avascular tumor, *Phys. Rev. E* 65 (2002) 021907. 1–8.
- [18] M. Scalerandi, B. Capogrosso Sansone, C. Benati, C.A. Condat, Competition effects in the dynamics of tumor cords, *Phys. Rev. E* 65 (2002) 051918. 1–10.
- [19] D.G. Mallet, L.G. De Pillis, A cellular automata model of tumor–immune system interactions, *J. Theoret. Biol.* 239 (2006) 334–350.
- [20] L.G. De Pillis, D.G. Mallet, A.E. Radunskaya, Spatial tumor–immune modeling, *Comput. Math. Methods Med.* 7 (2006) 159–176.
- [21] S.A. Menchón, R.A. Ramos, C.A. Condat, Modeling subspecies and the tumor–immune system interaction: Steps towards understanding therapy, *Physica A* 386 (2007) 713–719.
- [22] D. Wodarz, N.L. Komarova, *Computational Biology of Cancer*, World Scientific, Singapore, 2005.
- [23] G. Morstyn, W. Sheridan (Eds.), *Cell Therapy*, Cambridge UP, Cambridge, UK, 1996.
- [24] V.T. DeVita, S. Hellman, S.A. Rosenberg (Eds.), *Principles and Practice of Oncology*, Lippincott Williams & Wilkins, Philadelphia, 2005.
- [25] S.A. Rosenberg, The emergence of modern cancer immunotherapy, *Ann. Surg. Oncol.* 12 (2005) 1–3.
- [26] M.S. Meltzer, M.M. Stevenson, E.J. Leonard, Characterization of macrophage chemotaxins in tumor cell cultures and comparison with lymphocyte-derived chemotactic factors, *Cancer Res.* 37 (1977) 721–725.

- [27] N. Delens, E. Torreele, H. Savelkool, P. de Baetselier, L. Bouwens, Tumor-derived transforming growth factor – β 1 and interleukin – 6 are chemotactic for lymphokine-activated killer cells, *Int. J. Cancer* 57 (1994) 696–700.
- [28] A.M. Hicks, et al., Transferable anticancer innate immunity in spontaneous regression/complete resistance mice, *Proc. Natl. Acad. Sci. USA* 103 (2006) 7753–7758.
- [29] A. Brú, S. Albertos, J.A. LópezGarcía-Asenjo, I. Brú, Pinning of tumoral growth by enhancement of immune response, *Phys. Rev. Lett.* 92 (2004) 238101. 1–4.
- [30] C.A. Condat, B. CapogrossoSansone, P.P. Delsanto, M. Scalerandi, Modeling cancer growth, *Rec. Res. Dev. Biophys. Chem.* 2 (2001) 53–69.
- [31] S.A. Menchón, C.A. Condat, Cancer growth: Predictions of a realistic model, *Phys. Rev. E* 78 (2008) 022901. 1–4.
- [32] B. Capogrosso Sansone, P.P. Delsanto, M. Magnano, M. Scalerandi, Effects of anatomical constraints on tumor growth, *Phys. Rev. E* 64 (2001) 021903. 1–8.
- [33] S.A. Menchón, C.A. Condat, Modeling tumor cell shedding, *Eur. Biophys. J.* 38 (2009) 479–485.
- [34] P.P. Delsanto, M. Griffa, C.A. Condat, S. Delsanto, L. Morra, Bridging the gap between mesoscopic and macroscopic models: the case of multicellular tumor spheroids, *Phys. Rev. Lett.* 94 (2005) 148105. 1–4.
- [35] E.J. Goetzl, A.H. Tashjian Jr, R.H. Rubin, K.F. Austen, Production of a low molecular weight eosinophil polymorphonuclear leukocyte chemotactic factor by anaplastic squamous cell carcinomas of human lung, *J. Clin. Investigation* 61 (1978) 770–780.
- [36] J. Van Damme, P. Proost, J.-P. Lenaerts, G. Opdenakker G, Structural and functional identification of two human, tumor derived, monocyte chemotactic proteins (MCP-2 and MCP-3) belonging to the chemokine family, *J. Exp. Med.* 176 (1992) 59–65.
- [37] A. Wiedemann, D. Depoil, M. Faroudi, S. Valitutti, Cytotoxic T Lymphocytes kill multiple targets simultaneously via spatiotemporal uncoupling of lytic and stimulatory synapses, *Proc. Natl. Acad. Sci. USA* 103 (2006) 10985–10990.
- [38] D.E. Speiser, P. Romero, Molecularly defined vaccines for cancer immunotherapy, and protective T cell immunity, *Semin. Immunol.* 22 (2010) 144–154.
- [39] B.D. Curti, et al., Influence of interleukin-2 regimens on circulating populations of lymphocytes after adoptive transfer of anti-CD3-stimulated T cells: results from a phase I trial in cancer patients, *J. Immunother. Emphasis Tumor Immunol.* 19 (1996) 296–308.
- [40] R.E. Merchant, D.W. McVicar, L.H. Merchant, H.F. Young, Treatment of recurrent malignant glioma by repeated intracerebral injections of human recombinant interleukin-2 alone or in combination with systemic interferon-alpha. Results of a phase I clinical trial, *J Neurooncol.* 12 (1992) 75–83.
- [41] J.D. Murray, *Mathematical Biology*, Vol. I, third ed., Springer, New York, 2002.
- [42] E. Beretta, Y. Kuang, Geometric stability switch criteria in delay differential systems with delay dependent parameters, *SIAM J. Math. Anal.* 33 (2002) 1144–1165.
- [43] A. d’Onofrio, F. Gatti, P. Cerrai, L. Freschi, Delay-induced oscillatory dynamics of tumour-immune system interaction, *Math. Comp. Modelling* 51 (2010) 572–591.